DMD Fast Forward. Published on March 18, 2005 as doi:10.1124/dmd.105.003848

DMD #3848

ENZYME-SELECTIVE EFFECTS OF NITRIC OXIDE ON AFFINITY AND MAXIMUM VELOCITY OF VARIOUS RAT CYTOCHROMES P450

Ragini Vuppugalla and Reza Mehvar

School of Pharmacy, Texas Tech University Health Sciences Center, Amarillo, Texas (RV and RM)

Running Title: Enzyme-Selective Effects of Nitric Oxide on CYP450

Address Correspondence to: Reza Mehvar, Ph.D., School of Pharmacy, Texas Tech University Health Sciences Center, 1300 S. Coulter, Amarillo, TX 79106, Telephone: (806) 356-4015 Ext. 337, FAX: (806) 356-4034, E-Mail: reza.mehvar@ttuhsc.edu

Number of text pages: 18

Number of tables: 1

Number of figures: 7

Number of references: 38

Number of words in the

Abstract: 250

Introduction: 564

Discussion: 1668

ABBREVIATIONS: P450, cytochrome P450; iNOS, inducible nitric oxide synthase; NO, nitric oxide; IPRL, isolated perfused rat liver; MM, Michaelis-Menten; V_{max}, maximum velocity of metabolism; K_m, MM constant; Cl_{int}, intrinsic clearance; SNP, sodium nitroprusside; ISDN, isosorbide dinitrate; CLZ, chlorzoxazone; 6-HCLZ, 6-hydroxychlorzoxazone; DM, dextromethorphan; MXM, methoxymorphinan; DT, dextrorphan; R, resorufin; BR, benzyloxyresorufin; ER, ethoxyresorufin; T, testosterone; 6β-HT, 6β-hydroxytestosterone; 16α-HT, 16α-hydroxytestosterone; NO_x, nitrate/nitrite; v, rate of metabolism; [s], substrate concentration; n, Hill coefficient; Cl_{total}, total intrinsic clearance; Cl_{max}, maximum clearance.

DMD Fast Forward. Published on March 18, 2005 as DOI: 10.1124/dmd.105.003848
This article has not been copyedited and formatted. The final version may differ from this version.

ABSTRACT

Nitric oxide (NO) has recently been shown to decrease cytochrome P450 (P450) enzyme activity rapidly (≤ 30 min), concentration-dependently, and enzyme-selectively in the rat liver. Interestingly, among all the studied P450 enzymes, only CYP2D1 was not affected by NO donors. However, these studies were conducted using only a single concentration of the substrates, thus lacking information about the possible simultaneous changes in both maximum velocity (V_{max}) and affinity (K_m) of the enzymes. In the present study, we systematically evaluated the effects of NO on the enzyme kinetic parameters of marker substrates for a range of P450 enzymes, including 2D1. Livers were perfused (1 h) in the absence (Control) or presence of two NO donors with different mechanisms of NO release. At the end of the perfusion, microsomes were prepared and used for kinetic analysis. Except for 2D1, NO reduced the V_{max} of all the model reactions studied, although to a varying degree. However, the effects of NO donors on K_m were more diverse. Whereas the K_m values for testosterone 6β- (3A2) and 16α- (2C11) hydroxylation significantly decreased, the values for chlorzoxazone 6-hydroxylation (2E1), dextromethorphan N-demethylation (3A2), and high affinity ethoxyresorufin O-dealkylation (1A1/2) significantly increased in the presence of NO donors. Further, the K_m values for the high affinity component of dextromethorphan O-demethylation and benzyloxyresorufin O-dealkylation remained unchanged. These results indicate that NO can potentially change both the V_{max} and K_m of various substrates selectively and confirm our previous findings that the activity of CYP2D1 is not affected by NO donors.

Cytochrome P450 (P450) enzymes are heme-containing proteins critical to the metabolism and subsequent excretion of a large number of drugs and toxic agents as well as endogenous compounds. It is well established today that the ability of the liver to carry out P450-dependent drug biotransformation is compromised in patients with infectious diseases or disease states that are associated with inflammation (Morgan, 1997; Morgan, 2001; Renton, 2004; Riddick et al., 2004). Despite wide acceptance that the stimulation of immune system can inhibit drug metabolism, the exact mechanisms responsible for this down-regulation are still not well understood. Large quantities of cytokines, produced during inflammation, are believed to be responsible, at least in part, for mediating suppression of P450 enzymes at the transcriptional level (Morgan, 1997). Indeed, several reports (Ghezzi et al., 1986; Warren et al., 1999) have shown that the administration of inflammatory cytokines depresses P450 activities and contents both in vivo and in vitro.

In addition to cytokines, inflammatory states induce the expression of iNOS and result in excessive production of nitric oxide (NO) in both hepatocytes and Kupffer cells (Nathan, 1992). Although some reports (Sewer et al., 1998; Sewer and Morgan, 1998; Takemura et al., 1999) suggest that P450 enzyme down-regulation occurs independently of NO, others (Stadler et al., 1994; Khatsenko and Kikkawa, 1997; Khatsenko, 1998) have shown that NO may also play a role in this event. Besides these indirect evidence for an NO role in inflammation-induced P450 depression, attempts have also been made at delineating the effects of NO directly using NO donors in the microsomes or purified enzyme systems (Khatsenko et al., 1993; Wink et al., 1993; Minamiyama et al., 1997). Supporting the above findings, very recently (Vuppugalla and Mehvar, 2004a) we showed the inhibitory effects of NO on P450 to be rapid, concentration-dependent, and enzyme-selective in an isolated perfused rat liver (IPRL) model. Furthermore, we

also conducted the time course studies to assess the mechanisms responsible for the NO-mediated P450 inhibition and demonstrated that the short-term inhibitory effects of NO are time-dependent, consisting of both reversible and irreversible components (Vuppugalla and Mehvar, 2004b).

One of the novel findings of our IPRL studies (Vuppugalla and Mehvar, 2004a; Vuppugalla and Mehvar, 2004b) was the apparent lack of the effect of NO donors on CYP2D1 enzyme along with different degrees and time courses of inhibition or reversal of activities for other P450 enzymes. These studies were carried out only with a single substrate concentration. Therefore, one may argue that the observed enzyme-selective effects of NO may have been due to different positions of substrate concentrations along their respective Michaelis-Menten (MM) kinetic curves. This is especially true if NO alters both V_{max} and K_m of P450 enzymes. Although the interaction of NO with P450 heme (Kim et al., 1995) suggests a reduction in V_{max}, the possibility of alterations in K_m cannot be ruled out based on the available data. Additionally, the significance of NO-induced inhibition of P450 enzymes to the overall pharmacokinetics of a drug can be better appraised if the effects of NO on the P450 enzyme kinetic parameters (K_m, V_{max}, and Cl_{int}) are known. However, to the best of our knowledge, this information is not available in the literature. Thus, in the present study, we investigated the direct effects of NO donors sodium nitroprusside (SNP) and isosorbide dinitrate (ISDN) on the kinetic parameters of various P450 probe substrates using an IPRL model.

Materials and Methods

Materials. The following chemicals were purchased from Sigma-Aldrich (St. Louis, MO): SNP, ISDN, chlorzoxazone (CLZ), 6-hydroxychlorzoxazone (6-HCLZ), NADPH, $NADP^+$,

magnesium chloride, glucose 6-phosphate, glucose-6-phosphate dehydrogenase, dextromethorphan (DM), methoxymorphinan (MXM), dextrorphan (DT), resorufin (R), cortexolone, umbelliferone, isocitrate, and isocitrate dehydrogenase. Benzyloxyresorufin (BR) and ethoxyresorufin (ER) were purchased from Molecular Probes (Eugene, OR). Testosterone (T), 6β-hydroxytestosterone (6β-HT), and 16α-hydroxytestosterone (16α-HT) were purchased from Steraloids (Wilton, NH). All the other reagents were of analytical grade and obtained from commercial sources.

Animals. Male Sprague-Dawley rats weighing between 230-320 g were purchased from Charles River Laboratories, Inc. (Wilmington, MA). Animals were housed in a temperature- and humidity-controlled room under a 12-h light/dark cycle, with free access to food and water. Texas Tech Health Sciences Center Animal Care and Use Committee approved the study protocol, and all the animals received humane care in compliance with guidelines set by the National Institute of Health (publication no. 85-23, revised 1985, Bethesda, MD).

Liver Perfusion and Microsomal Preparation. The procedures for isolation of the livers, their ex vivo perfusion with NO donors, and subsequent preparation of microsomes have been reported in detail in our previous study (Vuppugalla and Mehvar, 2004a). Briefly, after isolation from untreated animals, livers were perfused for 1 h either in the absence (Control) or presence of 200 μM of SNP or ISDN (n = 4/group) in a single-pass mode. At the end of the perfusion, the livers were blotted dry, weighed, and subjected to the preparation of microsomes using well-established ultracentrifugation methods. Protein concentrations were measured by the Bradford method.

Measurement of P450 Enzyme Activities. In preliminary studies, all the assays were checked for linearity of rate of metabolism with respect to the incubation time and microsomal

protein concentrations. Additionally, substrate consumptions were determined at the lowest and highest substrate concentrations included in the study.

The activities of CYP3A2 and 2C11 were analyzed based on the formation of 6β- and 16α-hydroxytestosterone, respectively, from testosterone, based on our modification (Vuppugalla and Mehvar, 2004a) of a previously published method (Purdon and Lehman-McKeeman, 1997). The microsomal protein concentration and incubation time were 200 µg/ml and 10 min, respectively. The substrate (testosterone) concentrations were 10, 20, 50, 100, 200, and 300 µM.

The activity of CYP2E1 was measured based on the formation of 6-HCLZ from CLZ. A detailed description of the incubation conditions and high-performance liquid chromatographic analysis of the drug and the metabolite has been reported by us before (Vuppugalla and Mehvar, 2004a). The microsomal protein concentration and incubation time were 800 µg/ml and 15 min, respectively. The substrate (CLZ) concentrations were 5, 10, 25, 50, 100, 250, and 500 µM.

The activities of CYP2D1 and 3A2 were measured based on the formation of DT and MXM, respectively, from DM. The details of the procedure have been described by us before (Vuppugalla and Mehvar, 2004a). The microsomal protein concentration and incubation time were 500 µg/ml and 5 min, respectively. The substrate (DM) concentrations were 0.5, 2.5, 5, 10, 50, 100, 200, and 500 µM.

The activities of CYP2B1/2 and 1A1/2 were assessed based on the formation of resorufin from BR (Burke et al., 1985) and ER (Rutten et al., 1992), respectively. Rate of formation of resorufin was monitored fluorometrically based on a kinetic analysis over 150-300 sec of incubation, and the microsomal protein concentration was 200 µg/ml. The substrate

concentrations were 20, 40, 80, 160, 320, 1250, 2500, and 5000 nM for BR and 10, 20, 40, 80, 320, 625, 1250, and 2500 nM for ER.

Estimation of Microsomal Protein Binding. Binding of various substrates to microsomes was determined by an ultrafiltration technique. Samples contained the same concentration of microsomes and the lowest and highest substrate concentrations used in the kinetic study, described above. After incubation at 37ºC for indicated times, an aliquot was transferred into 10,000 kDa molecular weight cutoff filters (Centricon 10; Amicon, Danvers, MA) and centrifuged at 2000 g for 20 min. Subsequently, the substrate concentrations were determined in the filtrates and the initial samples.

Analysis of Nitrate/Nitrite (NO_x) in the Perfusate. The NO_x concentration in the outlet perfusate was measured using the Griess reagent (Active Motif, Carlsbad, CA) at the end of the 1-h perfusion with SNP or ISDN.

Data Analysis. The kinetic parameters were estimated based on nonlinear regression analysis using WinNonlin program (Pharsight, Mountain View, CA). Biotransformation of all the substrates was modeled using a subset of the following general equation:

$$v = \frac{V_{\max(1)}[S]^{n(1)}}{K_{m(1)}{}^{n(1)} + [S]^{n(1)}} + \frac{V_{\max(2)}[S]^{n(2)}}{K_{m(2)}{}^{n(2)} + [S]^{n(2)}} \quad (1)$$

where $V_{max(1)}$ and $K_{m(1)}$ are related to the high-affinity, low-capacity site, and $V_{max(2)}$ and $K_{m(2)}$ are the corresponding parameters for the second low-affinity, high-capacity site. This equation allows single- or dual-enzyme metabolite formation with or without sigmoidicity. In its simplest form, the equation is reduced to a classic hyperbolic Michaelis-Menten relationship, when the metabolite is formed by a single enzyme in the absence of sigmoidicity (i.e., n =1):

$$v = \frac{V_{\max}[S]}{K_m + [S]} \quad (2)$$

Other variations of Equation (1) tested were the single-enzyme model with sigmoidicity or sigmoidal Hill equation (i.e., n >1) and dual-enzyme models with no sigmoidicity, one simple and one sigmoidal enzyme kinetics, or both enzymes with sigmoidal kinetics.

Model selection was based on the examination of Eadie-Hofstee transformed plots (rate versus rate/[s]), which suggested a subset of Equation (1) (e.g., single- versus dual-enzyme models or presence or absence of sigmoidicity). Further model selection from the possible subsets was based on criteria that included: Akaike's information criterion (AIC), visual inspection of the fit, the random distribution of residuals, and the standard error of the parameter estimates. All fittings were carried out with a weight of $1/v$.

In the absence of sigmoidicity, the intrinsic clearance (Cl_{int}) value for each enzyme was calculated by dividing the corresponding enzyme V_{max} by its K_m. The total intrinsic clearance (Cl_{total}) was then determined by the summation of the individual Cl_{int} values:

$$Cl_{total} = Cl_{\mathrm{int}(1)} + Cl_{\mathrm{int}(2)} \qquad (3)$$

For sigmoidal models, Cl_{max}, which was obtained graphically from the clearance plot (rate/[s] versus [s] plot) (Houston and Kenworthy, 2000), was used instead of Cl_{int} or Cl_{total}.

In protein binding studies, the free fraction of substrate was estimated by dividing the substrate concentration in the filtrate to that in the unfiltered suspension.

All the statistical comparisons were conducted using ANOVA with subsequent Fisher's test for comparison of three groups or using an unpaired *t* test for comparison of two groups. All tests were conducted at a significance level of 0.05. Data are presented as mean ± S.E.M.

Results

Formation of metabolites from all the substrates studied was linear with respect to the selected incubation times and microsomal protein concentrations. Moreover, less than 20% of substrates were consumed during such incubations. In addition, the free (not bound to microsomal proteins) fractions of all the studied substrates were close to unity (≥0.85) under the conditions used in this study.

Biotransformation of testosterone to 6β-hydroxytestosterone, catalyzed by 3A2 enzyme displayed hyperbolic saturation kinetics in all the three groups studied (Control, SNP, and ISDN) (Fig. 1, top). Eadie-Hofstee plots of the data were monophasic (Fig. 1, bottom), indicating apparent single-enzyme kinetics without sigmoidicity. Kinetic parameters for the formation of this metabolite via 3A2 enzyme are reported in Table 1. Both the K_m and V_{max} values were significantly lower ($P < 0.05$) in the microsomes of the livers perfused with SNP or ISDN, compared with their respective controls (Table 1). The percentages of reduction in the K_m and V_{max} values were, respectively, 63% and 67% for SNP and 43% and 34% for ISDN. However, because of the simultaneous NO donor-induced declines in both V_{max} and K_m, the Cl_{int} values remained unchanged after treatment with either of NO donors.

Similar to the formation of 6β-hydroxytestosterone (3A2), the formation of 16α-hydroxytestosterone from testosterone by 2C11 was best described by a simple, single-enzyme model without any sigmoidicity (Fig. 2 and Table 1). Similarly, both SNP and ISDN treatments resulted in a decline in the K_m (~80%) and V_{max} (~60%) values (Table 1). In contrast to data for 3A2, however, the Cl_{int} increased after treatment with ISDN ($P < 0.05$) (Table 1).

Eadie-Hofstee plots for the formation of DT from DM, catalyzed primarily by CYP2D1 enzyme, displayed biphasic kinetics without sigmoidicity in all the groups studied (Fig. 3, lower

DMD Fast Forward. Published on March 18, 2005 as DOI: 10.1124/dmd.105.003848
This article has not been copyedited and formatted. The final version may differ from this version.

panel). Therefore, the kinetic parameters were obtained using a dual-enzyme Michaelis-Menten model with an n of 1 (Table 1). The kinetic parameters for the high-affinity component ($K_{m(1)}$, $V_{max(1)}$, and $Cl_{int(1)}$) of DT remained mostly unchanged after treatment with either SNP or ISDN (Table 1). In contrast, treatment with SNP or ISDN resulted in a significant ($P < 0.05$) increase in the $K_{m(2)}$ and a decrease in the $V_{max(2)}$ and $Cl_{int(2)}$ values for the low-affinity component (Table 1). However, the contribution of the $Cl_{int(2)}$ for the low-affinity enzyme to the Cl_{total} was <10%.

Unlike the formation of DT (2D1) (Fig. 3), formation of MXM from DM (3A2) was characterized by convex Eadie-Hofstee plots (Fig. 4, middle panel), suggesting a sigmoidal model. Nonlinear regression analysis further showed that the data are best described by a single-enzyme sigmoidal model (Table 1). Additionally, in contrast to the formation of DT (2D1), the MXM (3A2) kinetic parameters were significantly affected by the perfusion of livers with SNP or ISDN (Table 1); SNP and ISDN, respectively, resulted in 2.4 and 2.2 fold increases in K_m, 84% and 50% decreases in V_{max}, and 88% and 68% decreases in Cl_{max} values (Fig. 4 and Table 1). The values of Cl_{max} were obtained graphically (Fig. 4, bottom panel).

Various plots, depicting the kinetics of 6-HCLZ formation from CLZ are shown in Fig. 5. Formation of 6-HCLZ catalyzed primarily by CYP2E1 demonstrated homotropic activation (Fig. 5, middle panel) in both the control and ISDN groups, and this was best fit to a single-enzyme, sigmoidal model (i.e., Hill equation) (Table 1). In contrast, the SNP-treated group of livers displayed a clear biphasic pattern (Fig. 5, Eadie-Hofstee plot), with a low affinity component exhibiting a convex curvature and an additional linear high affinity component. Therefore, a two-enzyme model, consisting of a Michaelis-Menten (n = 1; high affinity) and Hill equation (n > 1; low affinity) best described this data (Table 1). This means that the SNP treatment resulted in the appearance of an additional high affinity, low capacity component ($K_{m(1)}$

DMD Fast Forward. Published on March 18, 2005 as DOI: 10.1124/dmd.105.003848
This article has not been copyedited and formatted. The final version may differ from this version.

and $V_{max(1)}$) that was not apparent for the Control and ISDN groups (Table 1). Therefore, only the kinetic parameters of the low affinity component of the SNP-treated microsomes were compared with those of the Control and ISDN groups (Table 1). Treatment with either SNP or ISDN resulted in 40-70% decreases in the $V_{max(2)}$ and the graphically-estimated (Fig. 5, bottom panel) Cl_{max} values (Table 1). However, the $K_{m(2)}$ value increased only by SNP pretreatment (Table 1).

The metabolic data for the formation of resorufin from BR (2B1/2) are reported in Table 1, and the corresponding plots are shown in Fig. 6. Although the Eadie-Hofstee plots were biphasic without sigmoidicity for both the Control and ISDN groups, the SNP group displayed sigmoidal kinetics (Fig. 6, Eadie-Hofstee plots). The kinetic parameters were, therefore, obtained by nonlinear regression analysis of metabolite versus substrate data, using a dual-enzyme model with (SNP group) or without (Control and ISDN groups) incorporation of the sigmoidicity into the low affinity, high capacity component (Table 1). For the high affinity component, only the $V_{max(1)}$ and, consequently, $Cl_{int(1)}$ values were reduced by 70% in the ISDN group; SNP did not affect this enzyme (Table 1). ISDN also reduced the V_{max} and Cl_{int} of the low affinity component ($V_{max(2)}$ and $Cl_{int(2)}$) by ~70%. Consequently, the Cl_{total} value was decreased by a factor of 3 by ISDN. The $V_{max(2)}$ and $K_{m(2)}$ values for the SNP group could not be compared with those of the Control group because of the use of different models. However, the Cl_{max} value for the SNP group was significantly ($P < 0.05$, t-test) lower than Cl_{total} for the Control group (Table 1).

The metabolic data for the formation of resorufin from ER (1A1/2) are presented in Fig. 7 and Table 1 for the Control and ISDN groups. Similar to the formation of DT from DM (2D1), these data were best described by a dual-enzyme model without sigmoidicity (Fig. 7 and Table 1). However, in the case of SNP, the fit for two of the microsomal preparations (out of four samples) was associated with large standard errors and unrealistic values. Therefore, the data for

DMD Fast Forward. Published on March 18, 2005 as DOI: 10.1124/dmd.105.003848
This article has not been copyedited and formatted. The final version may differ from this version.

the SNP treatment were not included in the analysis. As for ISDN, the treatment caused ~3 fold increase in $K_{m(1)}$, resulting in a proportional decrease in $Cl_{int(1)}$ (Table 1). On the other hand, both $K_{m(2)}$ and $V_{max(2)}$ significantly decreased, whereas $Cl_{int(2)}$ remained unaffected after ISDN treatment (Table 1). Nevertheless, ISDN caused a significant reduction in the Cl_{total} value for the formation of resorufin from ER (Table 1).

The NO_x concentrations in the outlet perfusate at the end of the 1-h perfusion with 200 μM SNP and ISDN were 10.2 ± 0.4 and 30.2 ± 2.5 μM, respectively.

Discussion

Recent reports have unequivocally demonstrated that NO reduces the activities of P450 enzymes directly, rapidly, and selectively in liver microsomes (Khatsenko et al., 1993; Wink et al., 1993; Minamiyama et al., 1997), hepatocytes (Stadler et al., 1994), and the intact liver (Vuppugalla and Mehvar, 2004a; Vuppugalla and Mehvar, 2004b). Several mechanisms including the reaction of NO with P450 heme, leading to its loss and degradation, and with apoprotein thiols were held responsible for the direct inhibitory effects of NO (Minamiyama et al., 1997; Vuppugalla and Mehvar, 2004b). While the former mechanism is expected to reduce the V_{max} of the enzyme, the latter may affect the binding of the substrates to the enzyme, thus changing the K_m value. Indeed, our present findings show, for the first time, that NO may alter both the K_m and V_{max} values of various P450 enzymes selectively (Table 1).

Whereas NO generally caused a reduction in V_{max}, it resulted in a decrease, increase, or no change in the K_m values of different enzymes (Table 1). The enzyme-selective magnitude of decreases in V_{max} may be due to differential accessibility of heme and/or cysteine thiolate of various enzymes (Gergel et al., 1997). NO can also form reversible nitrosyl-heme complexes in

DMD Fast Forward. Published on March 18, 2005 as DOI: 10.1124/dmd.105.003848
This article has not been copyedited and formatted. The final version may differ from this version.

the intact liver, which can potentially decrease the V_{max} of different enzymes selectively. However, as we demonstrated recently (Vuppugalla and Mehvar, 2004b), the ferric-NO complex could not be detected in our experimental design which requires preparation of microsomes. As for K_m, the reaction of NO with thiol groups of amino acid residues observed by us (Vuppugalla and Mehvar, 2004b) and others (Minamiyama et al., 1997) has been proposed as one of the mechanisms for the decrease in the enzyme activities by NO donors. Although not shown before experimentally, this suggests a decrease in the binding of the substrate to the enzyme, thus an increase in K_m. In agreement with this postulate, we also observed enzyme-selective increases in the K_m values for some enzymes (Table 1). Surprisingly, however, we also noticed a decrease in K_m for some reactions such as the formation of 6β- (3A2) and 16α- (2C11) hydroxytestosterone from testosterone and the low affinity component for the formation of resorufin from ER (1A1/2) (Table 1). This suggests that the previously reported (Minamiyama et al., 1997; Vuppugalla and Mehvar, 2004b) reaction of NO with the thiol groups of P450 apoprotein may facilitate the binding of substrates to some enzymes, thus expediting their metabolism. However, in all cases of the observed decrease in K_m, the V_{max} values were also decreased, such that the Cl_{int} values remained mostly unchanged in the presence of NO donors (Table 1).

In single-substrate concentration studies, we have recently (Vuppugalla and Mehvar, 2004b) shown that the activities of all the studied P450 enzymes, except for 2D1, were reduced by pretreatment of IPRLs with NO donors. The lack of effect of NO on 2D1 in these studies may have been due a simultaneous change in both the V_{max} and K_m values, not manifested as a change in activity at the particular substrate concentration selected. In agreement with earlier studies (Kerry et al., 1993; Witherow and Houston, 1999), the kinetics of DM O-demethylation in our study was best described by a two-site Michaelis-Menten model consisting of a high-affinity,

DMD Fast Forward. Published on March 18, 2005 as DOI: 10.1124/dmd.105.003848
This article has not been copyedited and formatted. The final version may differ from this version.

low-capacity and a low-affinity, high-capacity site. The high- and low-affinity K_m and V_{max} values of CYP2D1 activity in our control microsomes (Table 1) were also similar to those reported by these authors (Witherow and Houston, 1999). In our studies, the kinetic parameters of the high-affinity component ($K_{m(1)}$, $V_{max(1)}$, and $Cl_{int(1)}$), whose Cl_{int} contributed to 93% of the total intrinsic clearance, were not substantially affected by NO donors (Table 1). Only the high affinity component of the formation of DT from DM is attributed to the 2D1 enzyme (Kerry et al., 1993). Therefore, the apparent lack of NO effect on this component confirms the validity of the previous single-substrate concentration studies. It should be noted, however, that because of the small number of samples (n = 4) and substantial variability in the $Cl_{int(1)}$ data for DT formation in the control livers (Table 1), the power of our study to detect a small difference between Control and ISDN or SNP groups (Table 1), if indeed true, is low. Addition of three IPRL experiments to the control group resulted in a $Cl_{int(1)}$ value (µl/min/mg protein) of 620 ± 200 (n = 7), which is within 10% of the average values for the SNP (690 ± 230) and ISDN (630 ± 60) groups ($P > 0.05$). Although not conclusive, the closeness of the mean values in all three groups suggests that the lack of effect of NO donors on $Cl_{int(1)}$ for DT formation is likely real and not due to a low statistical power.

The apparent lack of effects of NO donors on 2D1 V_{max} is likely due to inaccessibility of heme and/or cysteine thiolate of this enzyme (Gergel et al., 1997). Additionally, the lack of effects of NO donors on the K_m value of this enzyme may be due to the lack of importance of thiol-containing amino acid (i.e., cysteine) residues in binding to the substrate. Indeed, recent reports (Paine et al., 2003) have clearly shown that the critical amino acids for the interaction of 2D6 with basic nitrogen-containing ligands are negatively-charged carboxylate-containing amino acids, such as Aspartate-301 and Glutamate-216, and not cysteine residues. Nevertheless, these

studies confirm that CYP2D1 is unique among the studied P450 enzymes in that it is not affected by NO donors.

In our present studies, the metabolic kinetics of 3A2 activity were determined by using both the 6β-hydroxylation of testosterone (Bogaards et al., 2000) and formation of MXM from DM (Witherow and Houston, 1999) (Table 1). Whereas the former did not show any sigmoidicity (Fig. 1), the latter demonstrated sigmoidal kinetics (Fig. 4 and Table 1). This sigmoidal pattern is indicative of autoactivation of the metabolism (Ekins et al., 1997), suggesting that binding of one substrate molecule facilitates the binding of the next molecule (Houston and Kenworthy, 2000). Other investigations of MXM formation (Witherow and Houston, 1999) have also shown sigmoidal kinetics, with a K_m value (81 μM), close to that observed in our controls (53 μM, Table 1). The absence of autoactivation kinetics for 6β-hydroxylation of testosterone would indicate that the autoactivation phenomenon depends on the substrate and/or substrate-enzyme interaction, as demonstrated before (Ekins et al., 1998).

It is interesting to note that although both 6β-hydroxytestosterone (Bogaards et al., 2000) and MXM (Witherow and Houston, 1999) formation are catalyzed by the same CYP3A2 enzyme, NO decreased the K_m for 6β-hydroxylation, whereas it increased the K_m for MXM formation (Table 1). The opposing effects of NO donors on the two reactions catalyzed by the same enzyme could arise because NO may elicit a conformational, electronic, and/or steric change in the enzyme that increases the testosterone's affinity for the catalytic site, but decreases the metabolism of DM to MXM. This effect has also been demonstrated earlier (Schwab et al., 1988) for the ability of α-naphthoflavone to directly inhibit or stimulate rabbit CYP3C enzyme, depending on the substrate employed.

Our results with regard to the enzyme models and the magnitude of kinetic parameters in Control microsomes (Table 1) are in agreement with the literature data for the formation of 6β-hydroxylation from testosterone via 3A2 (Bogaards et al., 2000), MXM from DM via 3A2 (Witherow and Houston, 1999), and DT from DM via 2D1 (Witherow and Houston, 1999). However, formation of 6-HCLZ from CLZ via 2E1 showed sigmoidicity in our Control microsomes (Fig. 5), a pattern not reported before (Jayyosi et al., 1995; Court et al., 1997; Bogaards et al., 2000; Howard et al., 2001). Despite this difference, the K_m values reported in these studies are close to that observed in our Control group (Table 1). As for resorufin formation from BR via 2B1/2, our two-enzyme kinetic model (Table 1) is different from the previously reported (Mayer et al., 1990) single-enzyme model. This discrepancy is most likely due to a narrower substrate concentration range employed by these investigators. Overall, most of our data and selected metabolic models for untreated microsomes are in agreement with the literature data.

Despite some quantitative differences between the effects of SNP and ISDN on the kinetic parameters of different substrates, qualitatively the two NO donors were similar in most cases (Table 1). One exception was the minor increase in the $V_{max(1)}$ for the formation of DT from DM in the presence of ISDN and not SNP (Table 1). Similar to the SNP group, however, this minor increase, which might be due experimental variability, did not result in a change in the $Cl_{int(1)}$ of the metabolic pathway.

In our previous (Vuppugalla and Mehvar, 2004a) and current studies, we used both SNP and ISDN, two NO donors with different mechanisms, sites, and modes of NO release (Feelisch, 1998), to assure that the observed P450 inhibitory effects are indeed due to the generation of NO and not related to nonspecific effects of these drugs. Whereas for SNP, a membrane-bound

enzyme is likely involved in the generation of NO in biological tissues, an NADPH-dependent cytochrome P450 pathway and an isoenzyme of the glutathione S-transferase family have been proposed for the bioactivation of organic nitrates. Additionally, the metabolism of ISDN, but not SNP, may generate NO_x independent of the formation of NO (Feelisch, 1998). Therefore, the perfusate level of NO_x after ISDN is likely an overestimation of the liver exposure to NO. In agreement with these observations, our recent study showed that despite producing higher perfusate NO_x concentrations at doses of 200 and 500 μM, the inhibitory effects of ISDN were less pronounced than those of SNP for most enzymes (Vuppugalla and Mehvar, 2004a). Nevertheless, the perfusate NO_x concentrations produced in our studies for ISDN (30.2 ± 2.4 μM) and SNP (10.2 ± 0.4 μM) are pathophysiologically relevant because they are well below the values reported in the plasma of liver transplant patients (Ioannidis et al., 1995) and endotoxemic animals (Li-Masters and Morgan, 2002) (250 and 800 μM, respectively).

Conclusions

In conclusion, our results show that the exposure of rat livers to pathophysiologically-relevant concentrations of NO causes marked alterations in the kinetic parameters of various P450 probe substrates. Whereas in most cases, the NO exposure causes a reduction in the V_{max} of the metabolic pathway, it may decrease, increase, or not change the K_m of the marker substrates. Moreover, in exception to all the studied P450 enzymes, NO did not affect any of the kinetic parameters of CYP2D1. Further studies on individual P450 enzymes are needed to determine the exact mechanisms responsible for the selective effects of NO on P450 enzymes.

References

Bogaards JJP, Bertrand M, Jackson P, Oudshoorn MJ, Weaver RJ, vanBladeren PJ, and Walther B (2000) Determining the best animal model for human cytochrome P450 activities: a comparison of mouse, rat, rabbit, dog, micropig, monkey and man. *Xenobiotica* **30:**1131-1152.

Burke MD, Thompson S, Elcombe CR, Halpert J, Haaparanta T, and Mayer RT (1985) Ethoxy-, pentoxy- and benzyloxyphenoxazones and homologues: a series of substrates to distinguish between different induced cytochromes P-450. *Biochem Pharmacol* **34:**3337-3345.

Court MH, Von Moltke LL, Shader RI, and Greenblatt DJ (1997) Biotransformation of chlorzoxazone by hepatic microsomes from humans and ten other mammalian species. *Biopharm Drug Dispos* **18:**213-226.

Ekins S, Ring BJ, Binkley SN, Hall SD, and Wrighton SA (1998) Autoactivation and activation of the cytochrome P450s. *Int J Clin Pharmacol Ther* **36:**642-651.

Ekins S, VandenBranden M, Ring BJ, and Wrighton SA (1997) Examination of purported probes of human CYP2B6. *Pharmacogenetics* **7:**165-179.

Feelisch M (1998) The use of nitric oxide donors in pharmacological studies. *Naunyn Schmiedebergs Arch Pharmacol* **358:**113-122.

Gergel D, Misik V, Riesz P, and Cederbaum AI (1997) Inhibition of rat and human cytochrome P4502E1 catalytic activity and reactive oxygen radical formation by nitric oxide. *Arch Biochem Biophys* **337:**239-250.

Ghezzi P, Saccardo B, Villa P, Rossi V, Bianchi M, and Dinarello CA (1986) Role of interleukin-1 in the depression of liver drug metabolism by endotoxin. *Infect Immun* **54:**837-840.

Houston JB and Kenworthy KE (2000) In vitro-in vivo scaling of CYP kinetic data not consistent with the classical Michaelis-Menten model. *Drug Metab Dispos* **28:**246-254.

Howard LA, Micu AL, Sellers EM, and Tyndale RF (2001) Low doses of nicotine and ethanol induce CYP2E1 and chlorzoxazone metabolism in rat liver. *J Pharmacol Exp Ther* **299:**542-550.

Ioannidis I, Hellinger A, Dehmlow C, Rauen U, Erhard J, Eigler FW, and De Groot H (1995) Evidence for increased nitric oxide production after liver transplantation in humans. *Transplantation* **59:**1293-1297.

Jayyosi Z, Knoble D, Muc M, Erick J, Thomas PE, and Kelley M (1995) Cytochrome P-450 2E1 is not the sole catalyst of chlorzoxazone hydroxylation in rat liver microsomes. *J Pharmacol Exp Ther* **273:**1156-1161.

Kerry NL, Somogyi AA, Mikus G, and Bochner F (1993) Primary and secondary oxidative metabolism of dextromethorphan. In vitro studies with female Sprague-Dawley and Dark Agouti rat liver microsomes. *Biochem Pharmacol* **45:**833-839.

Khatsenko O (1998) Interactions between nitric oxide and cytochrome P-450 in the liver. *Biochemistry (Mosc)* **63:**833-839.

Khatsenko O and Kikkawa Y (1997) Nitric oxide differentially affects constitutive cytochrome P450 isoforms in rat liver. *J Pharmacol Exp Ther* **280:**1463-1470.

Khatsenko OG, Gross SS, Rifkind AB, and Vane JR (1993) Nitric oxide is a mediator of the decrease in cytochrome P450-dependent metabolism caused by immunostimulants. *Proc Natl Acad Sci U S A* **90:**11147-11151.

Kim YM, Bergonia HA, Muller C, Pitt BR, Watkins WD, and Lancaster JR, Jr. (1995) Loss and degradation of enzyme-bound heme induced by cellular nitric oxide synthesis. *J Biol Chem* **270:**5710-5713.

Li-Masters T and Morgan ET (2002) Down-regulation of phenobarbital-induced cytochrome P4502B mRNAs and proteins by endotoxin in mice: independence from nitric oxide production by inducible nitric oxide synthase. *Biochem Pharmacol* **64:**1703-1711.

Mayer RT, Netter KJ, Heubel F, Hahnemann B, Buchheister A, Mayer GK, and Burke MD (1990) 7-Alkoxyquinolines: new fluorescent substrates for cytochrome P450 monooxygenases. *Biochem Pharmacol* **40:**1645-1655.

Minamiyama Y, Takemura S, Imaoka S, Funae Y, Tanimoto Y, and Inoue M (1997) Irreversible inhibition of cytochrome P450 by nitric oxide. *J Pharmacol Exp Ther* **283:**1479-1485.

Morgan ET (1997) Regulation of cytochromes P450 during inflammation and infection. *Drug Metab Rev* **29:**1129-1188.

Morgan ET (2001) Regulation of cytochrome P450 by inflammatory mediators: Why and how? *Drug Metab Dispos* **29:**207-212.

Nathan C (1992) Nitric oxide as a secretory product of mammalian cells. *FASEB J* **6:**3051-3064.

Paine MJI, McLaughlin LA, Flanagan JU, Kemp CA, Sutcliffe MJ, Roberts GCK, and Wolf CR (2003) Residues glutamate 216 and aspartate 301 are key determinants of substrate specificity and product Regioselectivity in cytochrome P450 2D6. *J Biol Chem* **278:**4021-4027.

Purdon MP and Lehman-McKeeman LD (1997) Improved high-performance liquid chromatographic procedure for the separation and quantification of hydroxytestosterone metabolites. *J Pharmacol Toxicol Methods* **37:**67-73.

Renton KW (2004) Cytochrome p450 regulation and drug biotransformation during inflammation and infection. *Curr Drug Metab* **5:**235-243.

Riddick DS, Lee C, Bhathena A, Timsit YE, Cheng P-Y, Morgan ET, Prough RA, Ripp SL, Miller KKM, Jahan A, and Chiang JYL (2004) Transcriptional suppression of cytochrome P450 genes by endogenous and exogenous chemicals. *Drug Metab Dispos* **32:**367-375.

Rutten AA, Falke HE, Catsburg JF, Wortelboer HM, Blaauboer BJ, Doorn L, van Leeuwen FX, Theelen R, and Rietjens IM (1992) Interlaboratory comparison of microsomal ethoxyresorufin and pentoxyresorufin O-dealkylation determinations: standardization of assay conditions. *Arch Toxicol* **66:**237-244.

Schwab GE, Raucy JL, and Johnson EF (1988) Modulation of rabbit and human hepatic cytochrome P-450-catalyzed steroid hydroxylations by alpha-naphthoflavone. *Mol Pharmacol* **33:**493-499.

Sewer MB, Barclay TB, and Morgan ET (1998) Down-regulation of cytochrome P450 mRNAs and proteins in mice lacking a functional NOS2 gene. *Mol Pharmacol* **54:**273-279.

Sewer MB and Morgan ET (1998) Down-regulation of the expression of three major rat liver cytochrome P450s by endotoxin in vivo occurs independently of nitric oxide production. *J Pharmacol Exp Ther* **287:**352-358.

Stadler J, Trockfeld J, Schmalix WA, Brill T, Siewert JR, Greim H, and Doehmer J (1994) Inhibition of cytochromes P4501A by nitric oxide. *Proc Natl Acad Sci U S A* **91:**3559-3563.

Takemura S, Minamiyama Y, Imaoka S, Funae Y, Hirohashi K, Inoue M, and Kinoshita H (1999) Hepatic cytochrome P450 is directly inactivated by nitric oxide, not by inflammatory cytokines, in the early phase of endotoxemia. *J Hepatol* **30:**1035-1044.

Vuppugalla R and Mehvar R (2004a) Hepatic disposition and effects of nitric oxide donors: rapid and concentration-dependent reduction in the cytochrome P450-mediated drug metabolism in isolated perfused rat livers. *J Pharmacol Exp Ther* **310:**718-727.

Vuppugalla R and Mehvar R (2004b) Short-term inhibitory effects of nitric oxide on cytochrome P450-mediated drug metabolism: time dependency and reversibility profiles in isolated perfused rat livers. *Drug Metab Dispos* **32:**1446-1454.

Warren GW, Poloyac SM, Gary DS, Mattson MP, and Blouin RA (1999) Hepatic cytochrome P-450 expression in tumor necrosis factor-alpha receptor (p55/p75) knockout mice after endotoxin administration. *J Pharmacol Exp Ther* **288:**945-950.

Wink DA, Osawa Y, Darbyshire JF, Jones CR, Eshenaur SC, and Nims RW (1993) Inhibition of cytochromes P450 by nitric oxide and a nitric oxide-releasing agent. *Arch Biochem Biophys* **300:**115-123.

Witherow LE and Houston JB (1999) Sigmoidal kinetics of CYP3A substrates: an approach for scaling dextromethorphan metabolism in hepatic microsomes and isolated hepatocytes to predict in vivo clearance in rat. *J Pharmacol Exp Ther* **290:**58-65.

LEGENDS FOR FIGURES

FIG. 1. Michaelis-Menten (top panel) and Eadie-Hofstee (bottom panel) plots of microsomal formation of 6β-hydroxytestosterone from testosterone. Microsomes were obtained after perfusing the livers for 1 h with a buffer free of NO donors (Control) or containing 200 μM of SNP or ISDN (n = 4/group). The symbols and solid lines represent the observed (mean ± S.E.M.) and model-predicted values, respectively.

FIG. 2. Michaelis-Menten (top panel) and Eadie-Hofstee (bottom panel) plots of microsomal formation of 16α-hydroxytestosterone from testosterone. Microsomes were obtained after perfusing the livers for 1 h with a buffer free of NO donors (Control) or containing 200 μM of SNP or ISDN (n = 4/group). The symbols and solid lines represent the observed (mean ± S.E.M.) and model-predicted values, respectively.

FIG. 3. Michaelis-Menten (top panel) and Eadie-Hofstee (bottom panel) plots of microsomal formation of DT from DM. Microsomes were obtained after perfusing the livers for 1 h with a buffer free of NO donors (Control) or containing 200 μM of SNP or ISDN (n = 4/group). The symbols and solid lines represent the observed (mean ± S.E.M.) and model-predicted values, respectively.

FIG. 4. Michaelis-Menten (top panel), Eadie-Hofstee (middle panel), and clearance (bottom panel) plots of microsomal formation of MXM from DM. Microsomes were obtained after perfusing the livers for 1 h with a buffer free of NO donors (Control) or containing 200 μM of

SNP or ISDN (*n* = 4/group). The symbols and solid lines represent the observed (mean ± S.E.M.) and model-predicted values, respectively.

FIG. 5. Michaelis-Menten (top panel), Eadie-Hofstee (middle panel), and clearance (bottom panel) plots of microsomal formation of 6-HCLZ from CLZ. Microsomes were obtained after perfusing the livers for 1 h with a buffer free of NO donors (Control) or containing 200 μM of SNP or ISDN (*n* = 4/group). The symbols and solid lines represent the observed (mean ± S.E.M.) and model-predicted values, respectively.

FIG. 6. Michaelis-Menten (top panel), Eadie-Hofstee (bottom panel), and clearance (bottom panel) plots of microsomal formation of resorufin from BR. Microsomes were obtained after perfusing the livers for 1 h with a buffer free of NO donors (Control) or containing 200 μM of SNP or ISDN (*n* = 4/group). The symbols and solid lines represent the observed (mean ± S.E.M.) and model-predicted values, respectively.

FIG. 7. Michaelis-Menten (top panel) and Eadie-Hofstee (bottom panel) plots of microsomal formation of resorufin from ER. Microsomes were obtained after perfusing the livers for 1 h with a buffer free of NO donors (Control) or containing 200 μM of ISDN (*n* = 4/group). The symbols and solid lines represent the observed (mean ± S.E.M.) and model-predicted values, respectively.

TABLE 1

Effects of NO donors on the kinetic parameters of P450 substrates

Microsomes were obtained after perfusion of isolated rat livers for 1 hr in the absence (Control) or presence of 200 μM of NO donors sodium nitroprusside (SNP) or isosorbide dinitrate (ISDN) (*n* = 4/group). Kinetic parameters were estimated using equations described in the text. Values are mean ± S.E.

Enzyme Substrate Metabolite	Groups	Kinetic Parameters									
		High Affinity Component				Low Affinity Component				Overall	
		$K_{m(1)}$[a]	$V_{max(1)}$[b]	$n_{(1)}$	$Cl_{int(1)}$[c]	$K_{m(2)}$[a]	$V_{max(2)}$[b]	$n_{(2)}$	$Cl_{int(2)}$[c]	Cl_{max}[c]	Cl_{total}[c]
3A2 T[d] 6β–HT[d]	Control	51 ± 2	5.5 ± 0.6	1	110 ± 12	-[e]	-[e]	-[e]	-[e]	-[e]	110 ± 12
	SNP	19 ± 2[*]	1.8 ± 0.3[*]	1	93 ± 12	-[e]	-[e]	-[e]	-[e]	-[e]	93 ± 12
	ISDN	29 ± 2[*]	3.6 ± 0.6[*]	1	130 ± 26	-[e]	-[e]	-[e]	-[e]	-[e]	130 ± 26
2C11 T[d] 16α-HT[d]	Control	37 ± 2	2.2 ± 0.3	1	60 ± 10	-[e]	-[e]	-[e]	-[e]	-[e]	60 ± 10
	SNP	8.5 ± 0.7[*]	0.78 ± 0.06[*]	1	92 ± 3	-[e]	-[e]	-[e]	-[e]	-[e]	92 ± 3
	ISDN	8.4 ± 1.5[*]	0.96 ± 0.01[*]	1	130 ± 20[*]	-[e]	-[e]	-[e]	-[e]	-[e]	130 ± 20[*]
2D1 DM[d] DT[d]	Control	0.91 ± 0.38	0.43 ± 0.06	1	860 ± 320	35 ± 4	2.0 ± 0.1	1	59 ± 8	-[e]	920 ± 320
	SNP	0.76 ± 0.19	0.41 ± 0.05	1	690 ± 230	99 ± 24[*]	0.25 ± 0.04[*]	1	3.2 ± 0.9[*]	-[e]	700 ± 230
	ISDN	1.0 ± 0.1	0.62 ± 0.02[*]	1	630 ± 60	90 ± 22	0.59 ± 0.03[*]	1	8.2 ± 2.5[*]	-[e]	640 ± 60
3A2 DM[d] MXM[d]	Control	54 ± 2	6.4 ± 0.4	1.3 ± 0.0	-[e]	-[e]	-[e]	-[e]	-[e]	74 ± 3	-[e]
	SNP	130 ± 13[*]	1.0 ± 0.2[*]	1.3 ± 0.0	-[e]	-[e]	-[e]	-[e]	-[e]	9.1 ± 1.1[*]	-[e]
	ISDN	120 ± 13[*]	3.2 ± 0.2*	1.1 ± 0.1[*]	-[e]	-[e]	-[e]	-[e]	-[e]	24 ± 3[*]	-[e]
2E1 CLZ[d] 6-HCLZ[d]	Control	-[e]	-[e]	-[e]	-[e]	140 ± 8	1.9 ± 0.1	1.2 ± 0.0	-[e]	8.8 ± 0.4	-[e]
	SNP	4.6 ± 2.5	0.022 ± 0.006	1	7.7 ± 2.3	390 ± 40[*]	0.72 ± 0.11[*]	1.4 ± 0.1	-[e]	2.8 ± 0.2[*]	-[e]
	ISDN	-[e]	-[e]	-[e]	-[e]	190 ± 8	1.2 ± 0.1[*]	1.2 ± 0.0	-[e]	4.7 ± 0.5[*]	-[e]
2B1/2 BR[d] R[d]	Control	0.081 ± 0.019	2.9 ± 0.6	1	36 ± 2	1.5 ± 0.2	26 ± 3	1	19 ± 3	-[e]	54 ± 3
	SNP	0.086 ± 0.003	2.8 ± 0.2	1	32 ± 2	0.54 ± 0.06	12 ± 2	5.8 ± 0.2	-[e]	36 ± 3	-[e]
	ISDN	0.085 ±0.016	0.86 ± 0.15[*]	1	11 ± 2[*]	1.6 ± 0.3	8.1 ± 0.5[**]	1	6.0 ± 1.4[*]	-[e]	17 ± 3[**]
1A1/2 ER[d] R[d]	Control	0.014 ± 0.002	4.6 ± 0.9	1	330 ± 48	0.63 ± 0.03	67 ± 9	1	110 ± 18	-[e]	440 ± 65
	ISDN	0.044 ± 0.01[**]	4.5 ± 1.2	1	130 ± 45[**]	0.076 ± 0.01[**]	8.7 ± 2.8[**]	1	110 ± 33	-[e]	230 ± 42[**]

[a] Expressed as μM.

[b] Except for CYP2B1/2 and 1A1/2, which are expressed as pmol/mg protein/min, rates are expressed as nmol/mg protein/min.

[c] Expressed as μl/min/mg protein.

[d] T, testosterone; 6β–HT, 6β̃hydroxytestosterone; 16α–HT, 16α-hydroxytestosterone; DM, dextromethorphan; DT, dextrorphan; MXM, methoxymorphinan; CLZ, chlorzoxazone; 6-HCLZ, 6-hydroxy CLZ; BR, benzyloxyresorufin; R, resorufin; ER, ethoxyresorufin.

[e] Not applicable to the selected model.

[*] Significantly different from control: $P < 0.05$, ANOVA, followed by Fisher's test.

[**] Significantly different from control: $P < 0.05$, unpaired *t* test.

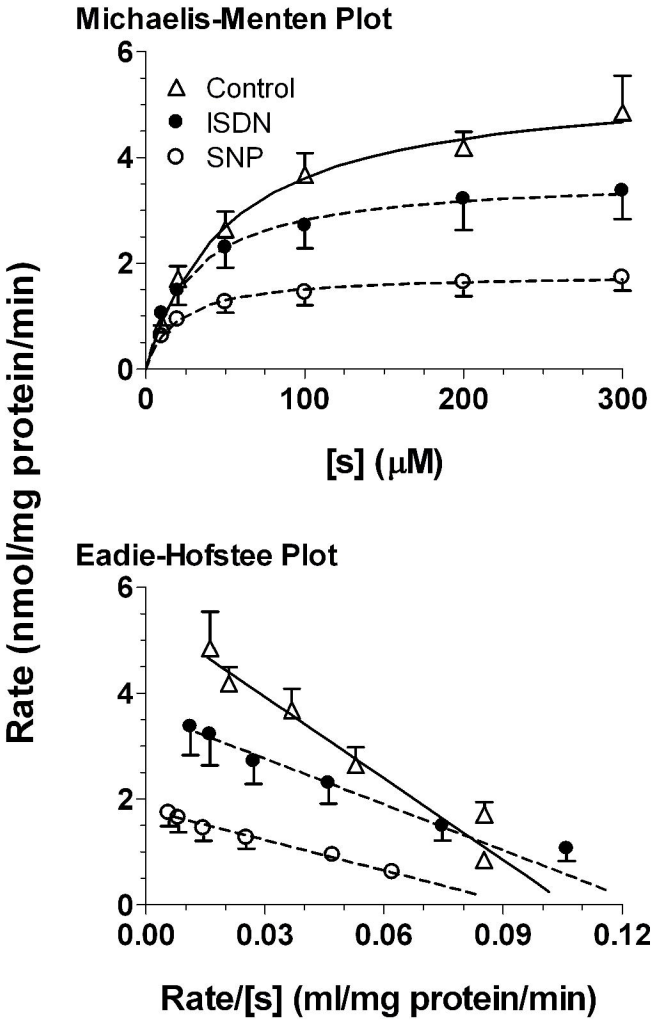
Michaelis-Menten Plot
Control
ISDN
SNP
Rate (nmol/mg protein/min)
[s] (μM)
Eadie-Hofstee Plot
Rate/[s] (ml/mg protein/min)

FIG. 1

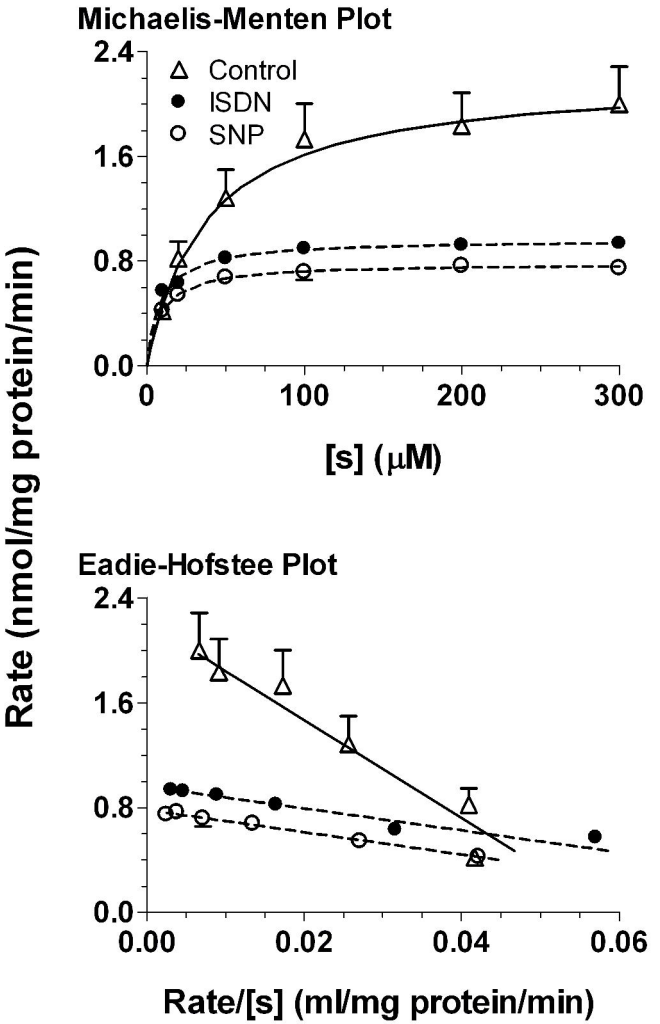
Michaelis-Menten Plot
Control
ISDN
SNP
2.4
1.6
0.8
0.0
0
100
200
300
[s] (μM)
Rate (nmol/mg protein/min)
Eadie-Hofstee Plot
2.4
1.6
0.8
0.0
0.00
0.02
0.04
0.06
Rate/[s] (ml/mg protein/min)

FIG. 2

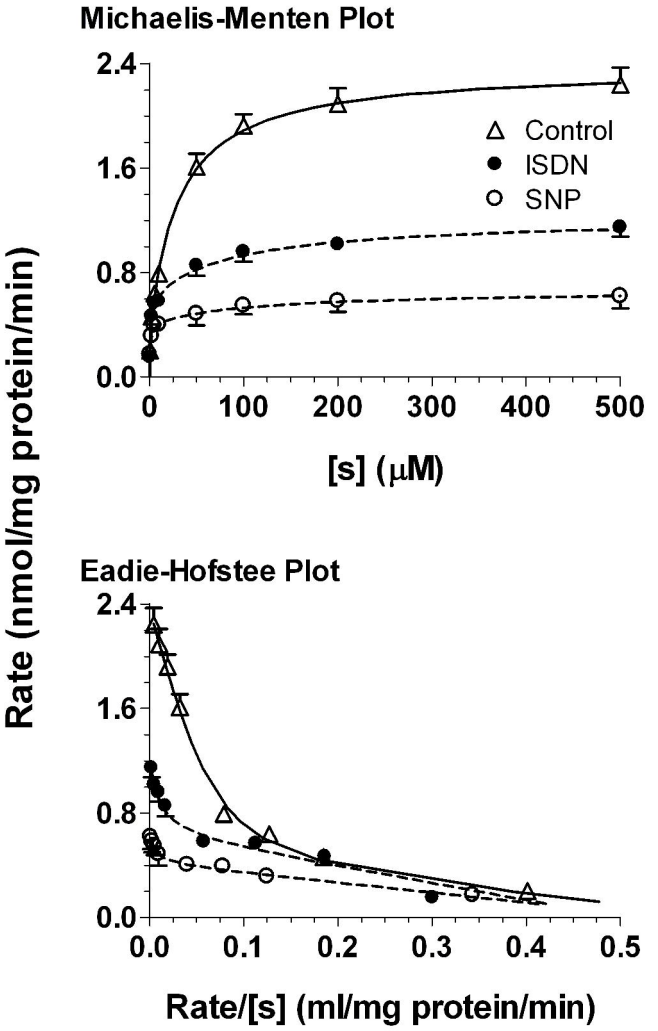
Michaelis-Menten Plot
2.4
1.6
0.8
0.0
0
100
200
300
400
500
Control
ISDN
SNP
[s] (μM)
Rate (nmol/mg protein/min)
Eadie-Hofstee Plot
2.4
1.6
0.8
0.0
0.0
0.1
0.2
0.3
0.4
0.5
Rate/[s] (ml/mg protein/min)

FIG. 3

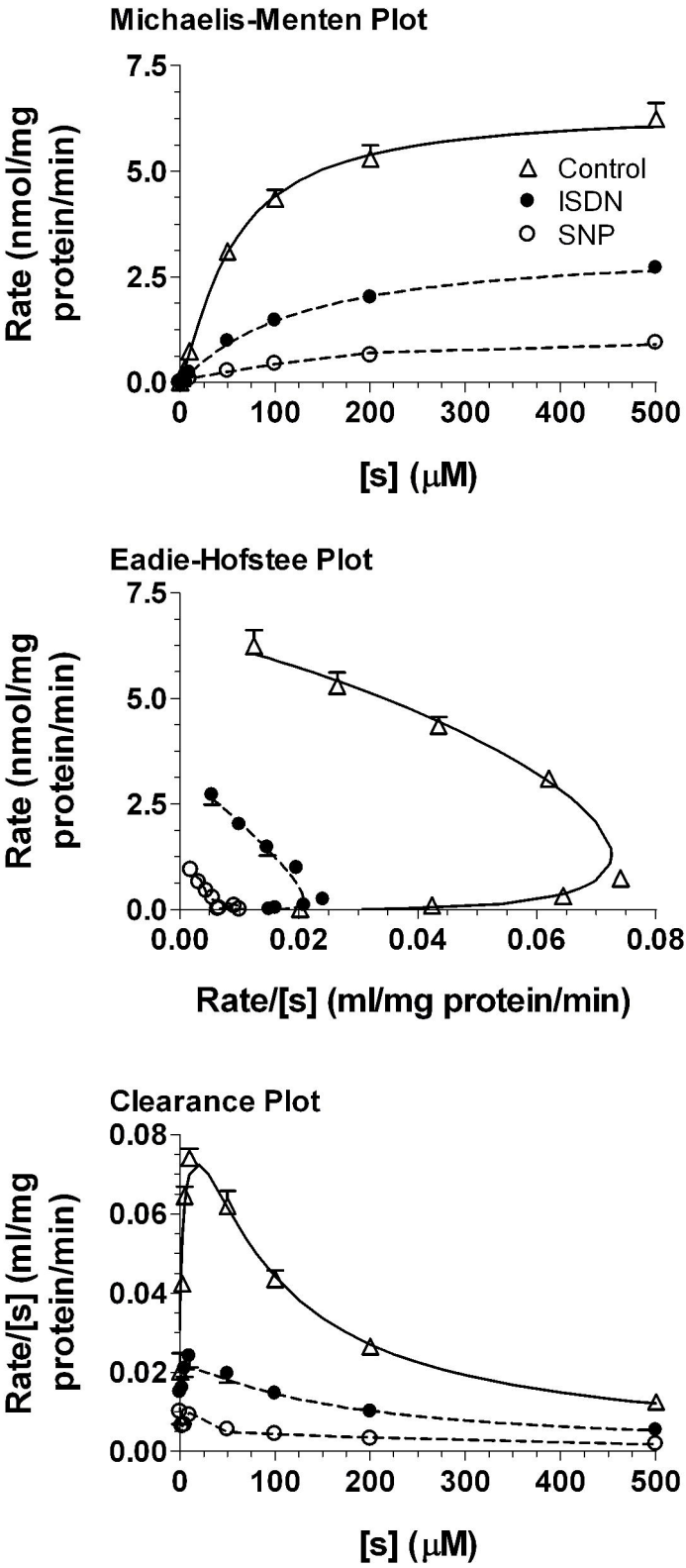
Michaelis-Menten Plot
Rate (nmol/mg protein/min)
7.5
5.0
2.5
0.0
Control
ISDN
SNP
0
100
200
300
400
500
[s] (μM)
Eadie-Hofstee Plot
Rate (nmol/mg protein/min)
7.5
5.0
2.5
0.0
0.00
0.02
0.04
0.06
0.08
Rate/[s] (ml/mg protein/min)
Clearance Plot
Rate/[s] (ml/mg protein/min)
0.08
0.06
0.04
0.02
0.00
0
100
200
300
400
500
[s] (μM)

FIG. 4

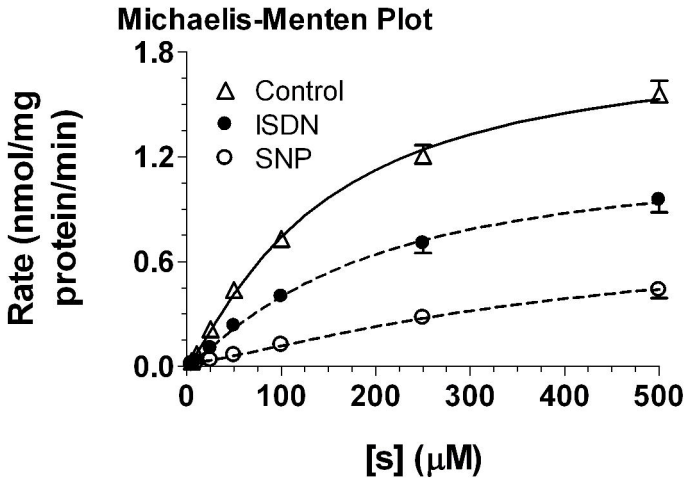
Michaelis-Menten Plot
Rate (nmol/mg protein/min)
1.8
1.2
0.6
0.0
Control
ISDN
SNP
0
100
200
300
400
500
[s] (μM)

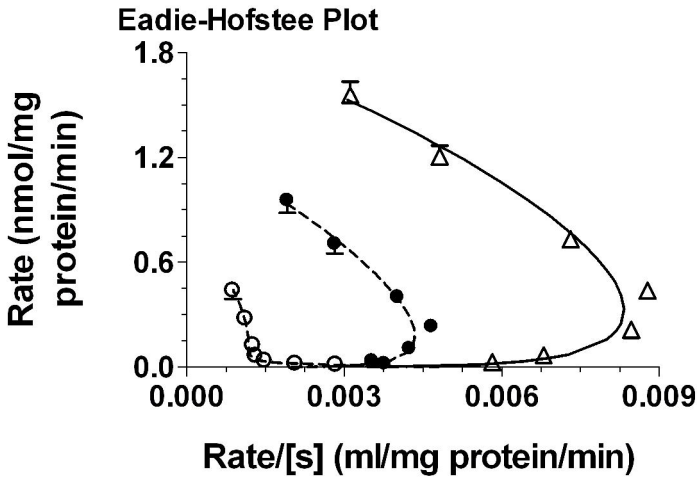
Eadie-Hofstee Plot
Rate (nmol/mg protein/min)
1.8
1.2
0.6
0.0
0.000
0.003
0.006
0.009
Rate/[s] (ml/mg protein/min)

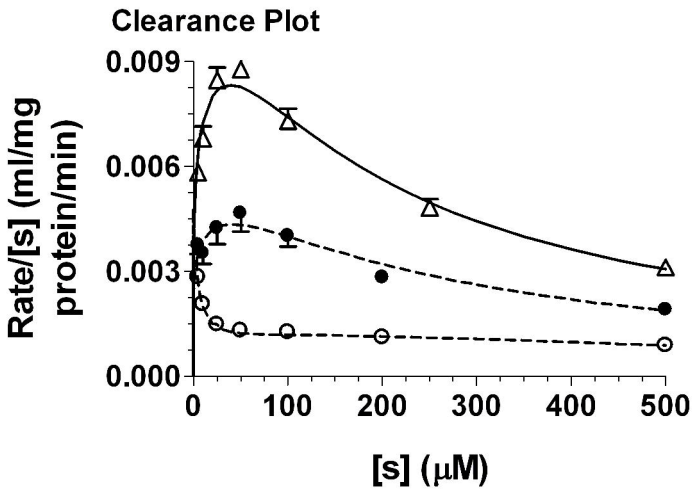
Clearance Plot
Rate/[s] (ml/mg protein/min)
0.009
0.006
0.003
0.000
0
100
200
300
400
500
[s] (μM)

FIG. 5

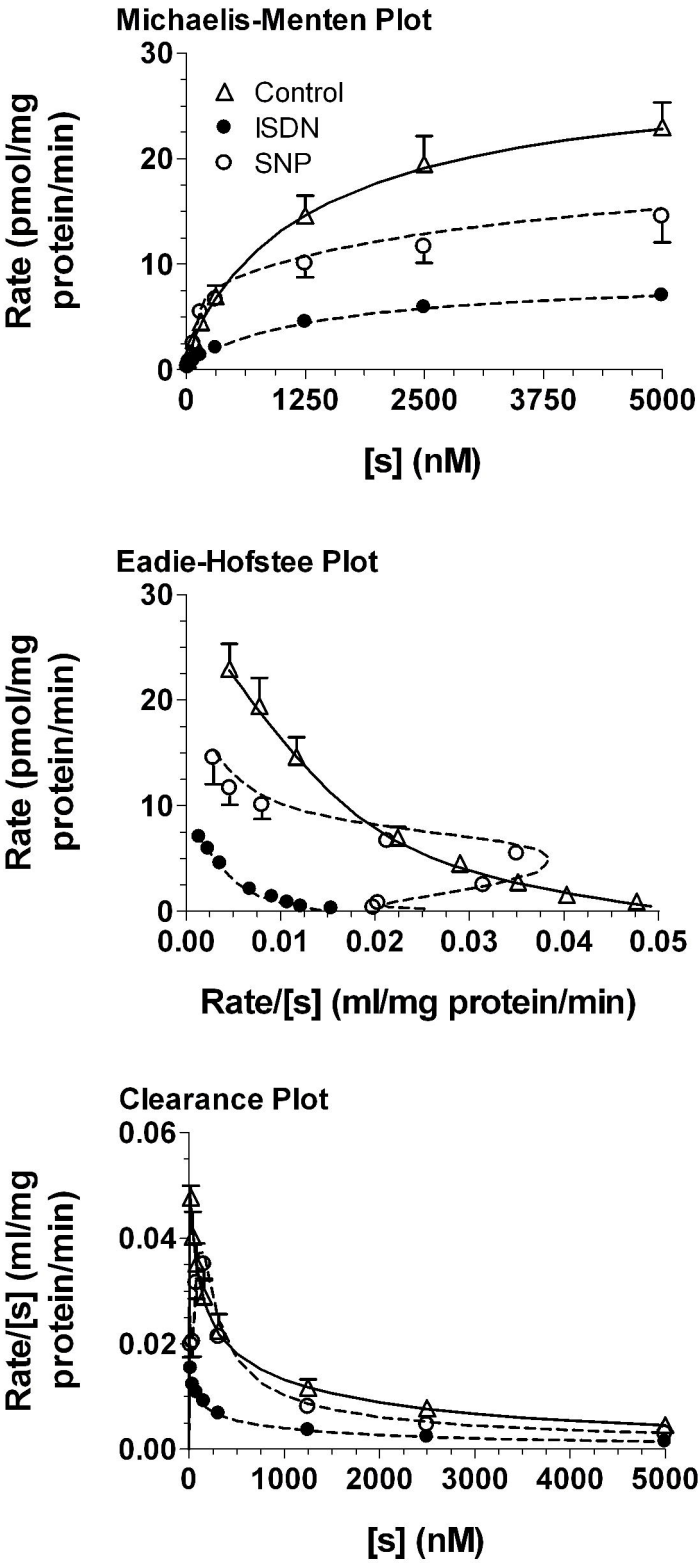
Michaelis-Menten Plot
Rate (pmol/mg protein/min)
30
20
10
0
Control
ISDN
SNP
0
1250
2500
3750
5000
[s] (nM)
Eadie-Hofstee Plot
Rate (pmol/mg protein/min)
30
20
10
0
0.00
0.01
0.02
0.03
0.04
0.05
Rate/[s] (ml/mg protein/min)
Clearance Plot
Rate/[s] (ml/mg protein/min)
0.06
0.04
0.02
0.00
0
1000
2000
3000
4000
5000
[s] (nM)

FIG. 6

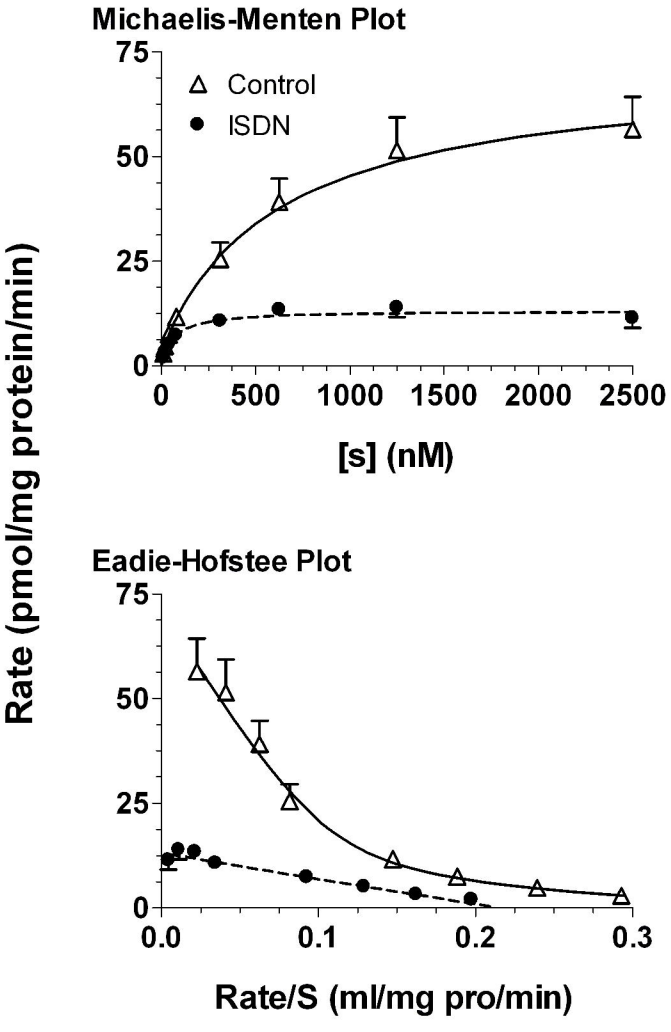
Michaelis-Menten Plot
75
50
25
0
Control
ISDN
0
500
1000
1500
2000
2500
[s] (nM)
Rate (pmol/mg protein/min)
Eadie-Hofstee Plot
75
50
25
0
0.0
0.1
0.2
0.3
Rate/S (ml/mg pro/min)

FIG. 7